32nd URSI GASS, Montreal, 19–26 August 2017

A Mechanism for Evolution of Electrostatic Solitary Waves in the Lunar Wake

R. Rubia*, S. V. Singh, and G. S. Lakhina
Indian Institute of Geomagnetism, New Panvel (West), Navi Mumbai, India - 410218

Abstract

Electrostatic waves have been observed in the lunar wake during the first flyby of the ARTEMIS mission on 13 February 2010. A mechanism for the generation of these electrostatic waves in terms of slow and fast ion-acoustic and electron-acoustic solitons is proposed. The lunar wake plasma is modelled by a four-component plasma system comprising of hot protons, hot heavier (He^{++}) ions, electron beam and suprathermal electrons having a κ-distribution. The analysis is based on multifluid equations and the Poisson equation, and uses the Sagdeev pseudopotential technique to study the arbitrary amplitude electrostatic solitary waves (ESWs). Three modes, viz., slow and fast ion-acoustic modes and electron-acoustic modes exist. The effect of beam velocity on the evolution of all three modes as well as their existence domain is explored. For the parameters considered, the electron-acoustic mode supports only the negative potential solitons. While both slow and fast ion-acoustic modes are found to support both positive and negative potential solitons as well as the coexistence of both polarities. In addition, both the ion-acoustic modes support a forbidden gap. The electric field amplitude of the bipolar solitary waves is found to be in the range $\sim (0.001-17)$ mV m^{-1} which is in excellent agreement with the observed value of $\sim (5-15)$ mV m^{-1}. The fast Fourier transform (FFT) of soliton electric fields generate broadband spectra having peak frequencies (corresponding to peak in the power spectra) in the range of $\sim (6.79-439.54)$ Hz, which corresponds to $\sim (0.002-0.14) f_{pe}$, where f_{pe} is the electron plasma frequency. This matches with the observed frequency $\sim (0.01-0.4) f_{pe}$.

1 Introduction

When the solar wind interacts with the moon, solar wind plasmas are absorbed by the moon, resulting in a depleted wake region in the nightside. The absence of intrinsic magnetic field and sufficiently low conductivity of the moon facilitates the easy penetration of the solar wind magnetic field through the moon as compared to the solar wind particles. The solar wind plasma refills the lunar wake along magnetic field lines due to the density gradient between the lunar wake and the solar wind. Ions and electrons undergo ambipolar diffusion during the refilling. Electrons being lighter rushes into the wake region ahead of the ions resulting in a negatively charged wake region. The potential gradient in the wake results in an ambipolar electric field that accelerates the ions into the wake [1].

Hashimoto et al. [2] substantiated the existence of ESWs in the lunar wake on the basis of the observations made by KAGUYA spacecraft. Tao et al. [1] provided a detailed analysis of the electrostatic waves in the lunar wake observed by the ARTEMIS mission during its first lunar wake flyby. These observations have motivated the study of ESWs in both unmagnetized and magnetized plasma involving suprathermal ions/electrons [3-4]. Tao et al. [1] considered a four-component model comprised of protons, ions, electron beam and suprathermal electrons. Both the electron beam and suprathermal electrons were considered to follow κ-distribution. They reported that the mode of the electrostatic waves observed in the lunar wake as the electron beam mode.

In this paper, we propose an alternative mechanism for the generation of electrostatic waves observed in the lunar wake [1] in terms of ion- and electron-acoustic solitons. The lunar wake plasma model comprises of hot protons, hot heavier (He^{++}) ions, electron beam and κ-distributed suprathermal electrons. Further, the existence domains of slow and fast ion-acoustic solitons and electron-acoustic solitons are examined as a function of the electron beam velocity.

2 Theoretical Model

The lunar wake plasma is modelled by a homogeneous, collisionless, and magnetized four-component plasma comprising of hot protons, hot heavier ions, i.e., alpha particles (He^{++}), electron beam and suprathermal electrons following κ-distribution given by [5]:

$$f_e(v) = \frac{N_{e0}}{\sqrt{\pi}\theta} \frac{\Gamma(\kappa+1)}{\kappa^{3/2}\,\Gamma(\kappa-1/2)} \left(1+\frac{v^2}{\kappa\theta^2}\right)^{-(\kappa+1)} \quad (1)$$

Here, $\Gamma(\kappa)$ is the gamma function, κ is the spectral index with $\kappa > 3/2$, and θ is the modified electron thermal speed given by

$$\theta^2 = \left(2-\frac{3}{\kappa}\right)\frac{T_e}{m_e}$$

Here, N_{e0} is the equilibrium number density of electrons. T_e and m_e are the temperature and mass of electrons, respectively. The ESWs are considered to be propagating parallel to the ambient magnetic field. The governing normalized multifluid equations are:

Continuity equation

$$\frac{\partial n_j}{\partial t} + \frac{\partial (n_j v_j)}{\partial x} = 0 \tag{2}$$

Momentum equation

$$\frac{\partial v_j}{\partial t} + v_j \frac{\partial v_j}{\partial x} + Z_j \mu_{pj} \frac{\partial \phi}{\partial x} + 3\mu_{pj}\sigma_j \frac{n_j}{n_{j0}^2} \frac{\partial n_j}{\partial x} = 0 \tag{3}$$

Poisson's equation

$$\frac{\partial^2 \phi}{\partial x^2} = (n_e + n_b - n_p - Z_i n_i) \tag{4}$$

In equations (2)-(4), the number densities are normalized by total equilibrium number density, $N_0 = N_{p0} + Z_i N_{i0} = N_{e0} + N_{b0}$, velocities are normalized with the ion-acoustic speed, $C_a = \sqrt{T_e/m_p}$, lengths with the effective hot electron Debye length, $\lambda_{de} = \sqrt{T_e/4\pi N_0 e^2}$, time with the inverse of the effective proton plasma frequency, $f_{pp} = \sqrt{4\pi N_0 e^2/m_p}$ and electrostatic potential, ϕ by T_e/e. Here, $\mu_{pj} = m_p/m_j$, where m_p is the mass of the proton and m_j is the mass of the j^{th} species. $\sigma_j = T_j/T_e$ and $n_{j0} = N_{j0}/N_0$ is the normalized equilibrium number density of j^{th} species. e is the electronic charge. v_j is the normalized fluid velocity. $Z_j = +1$ for protons, $Z_j = +2$ for heavier ions (alpha particles), $Z_j = -1$ for beam electrons. We have considered the adiabatic index $\gamma_j = 3$ for all species. This is justified for a one-dimensional case considered here. The above set of equations are transformed to a stationary frame moving with velocity V, the phase velocity of the electrostatic solitary wave, i.e., $\xi = x - Mt$, where $M = V/C_a$ is the Mach number. These equations are solved along with appropriate boundary conditions to obtain the expression for Sagdeev pseudopotential given by

$$\begin{aligned}
S(\phi,M) &= \frac{n_{p0}}{6\sqrt{3\sigma_p}}\left[\left(M+\sqrt{3\sigma_p}\right)^3 - \left\{\left(M+\sqrt{3\sigma_P}\right)^2 - 2\phi\right\}^{3/2} - \left(M-\sqrt{3\sigma_p}\right)^3 + \left\{\left(M-\sqrt{3\sigma_p}\right)^2 - 2\phi\right\}^{3/2}\right] \\
&+ \frac{n_{i0}}{6\sqrt{3\sigma_i}}\left\{\left(\frac{M}{\sqrt{\mu_{pi}}}+\sqrt{3\sigma_i}\right)^3 - \left[\left(\frac{M}{\sqrt{\mu_{pi}}}+\sqrt{3\sigma_i}\right)^2 - 2Z_i\phi\right]^{3/2} - \left(\frac{M}{\sqrt{\mu_{pi}}}-\sqrt{3\sigma_i}\right)^3 + \right. \\
&\left.\left[\left(\frac{M}{\sqrt{\mu_{pi}}}-\sqrt{3\sigma_i}\right)^2 - 2Z_i\phi\right]^{3/2}\right\} + \frac{n_{b0}}{6\sqrt{3\sigma_b}}\left\{\left(\frac{M-V_{b0}}{\sqrt{\mu_{pe}}}+\sqrt{3\sigma_b}\right)^3 - \left[\left(\frac{M-V_{b0}}{\sqrt{\mu_{pe}}}+\sqrt{3\sigma_b}\right)^2 + 2\phi\right]^{3/2}\right. \\
&\left. + \left[\left(\frac{M-V_{b0}}{\sqrt{\mu_{pe}}}-\sqrt{3\sigma_b}\right)^2 + 2\phi\right]^{3/2} - \left(\frac{M-V_{b0}}{\sqrt{\mu_{pe}}}-\sqrt{3\sigma_b}\right)^3\right\} + n_{e0}\left[1 - \left(1 - \frac{\phi}{\kappa - 3/2}\right)^{-\kappa+3/2}\right]
\end{aligned} \tag{5}$$

For the existence of soliton solutions, the Sagdeev pseudopotential $S(\phi,M)$ must satisfy the following conditions: (i) $S(\phi,M) = 0$, $dS(\phi,M)/d\phi = 0$, and $d^2S(\phi,M)/d\phi^2 < 0$ at $\phi = 0$, (ii) $S(\phi,M) = 0$ at $\phi = \phi_{max}$ (ϕ_{max} is the maximum attainable amplitude of the soliton), and (iii)$S(\phi,M) < 0$ for $0 < |\phi| < |\phi_{max}|$. When these conditions are satisfied, we obtain solitary wave solution.

The critical Mach number, M_0, above which soliton solution exists, satisfies the following equation:

$$\frac{n_{p0}}{M^2 - 3\sigma_p} + \frac{n_{i0}{Z_i}^2}{\frac{M^2}{\mu_{pi}} - 3\sigma_i} + \frac{n_{b0}}{\frac{(M-V_{b0})^2}{\mu_{pe}} - 3\sigma_b} = n_{e0}\left(\frac{2\kappa - 1}{2\kappa - 3}\right) \tag{6}$$

Solving the above equation for M_0 gives three positive physical roots. The lowest and the highest value of the three roots is designated as slow ion-acoustic mode and electron-acoustic mode, respectively. While the intermediate root corresponds to the fast ion-acoustic mode.

3 Numerical Results and Discussions

Figure 1 shows the existence curve for the slow ion-acoustic soliton as a function of V_{b0} for the normalized parameters: $n_{i0} = 0.05$, $n_{b0} = 0.02$, $\sigma_p = 0.3$, $\sigma_i = 0.5$, $\sigma_b = 0.002$, and $\kappa = 6$. In region-I, $0 \leq V_{b0} < 4$, we observe positive potential solitons, followed by negative potential solitons in region-II, $4 \leq V_{b0} < 5.4$. Region- III, $5.4 \leq V_{b0} < 6.1$ corresponds to the forbidden gap. Forbidden gap is the region over which the solitons cannot propagate. This is followed by a region of coexistence of both polarity solitons (region-IV, $6.1 \leq V_{b0} \leq 7$) lying between the two red-dashed lines. Here, the pink circles and green + signs shows the existence of negative and positive potential solitons, respectively. For $V_{b0} > 7$, we have positive potential solitons (Region-V). The limitation on the maximum attainable amplitude of the slow ion-acoustic positive polarity soliton is provided by the requirement that the number density of ions, n_i, should remain real, while for negative polarity solitons the limitation is provided by the number density of beam electrons, n_b.

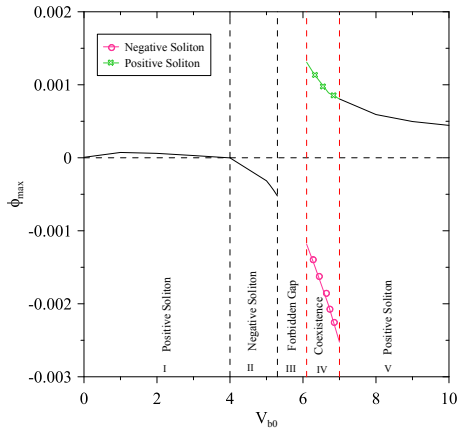

Figure 1. Existence domains of slow ion-acoustic soliton are depicted as a function of V_{b0} for the normalized parameters: $n_{i0} = 0.05$, $n_{b0} = 0.02$, $\sigma_p = 0.3$, $\sigma_i = 0.5$, $\sigma_b = 0.002$, and $\kappa = 6$.

Figure 2 shows the existence curve for the fast ion-acoustic soliton with respect to V_{b0} for the normalized parameters: $n_{i0} = 0.05$, $n_{b0} = 0.02$, $\sigma_p = 0.3$, $\sigma_i = 0.5$, $\sigma_b = 0.002$, and $\kappa = 6$. In region-I, $0 \leq V_{b0} < 5$, we observe positive potential solitons, followed by negative potential solitons in region-II, $5 \leq V_{b0} < 6.1$. This is followed by a forbidden gap in region-III ($6.1 \leq V_{b0} < 11$). Region-IV, $11 \leq V_{b0} < 12$, corresponds to the negative potential solitons. The region between the two red-dashed lines (Region-V, $12 \leq V_{b0} \leq 19$) corresponds to the coexistence of both polarity solitons. Here, the pink circles and blue + signs shows the existence of negative and positive potential solitons, respectively. For $V_{b0} > 19$, we have positive potential solitons (Region-VI). The maximum attainable amplitude of the positive polarity fast ion-acoustic soliton is limited by the requirement of the number density of protons, n_p, to remain real. For negative potential fast ion-acoustic soliton the amplitude is limited by the number density of beam electron, n_b.

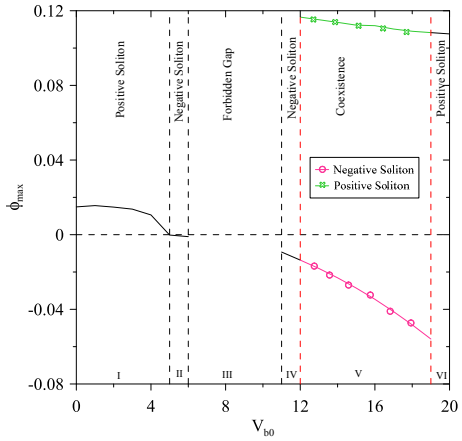

Figure 2. Existence domains of fast ion-acoustic soliton are depicted as a function of V_{b0} for the normalized parameters: $n_{i0} = 0.05$, $n_{b0} = 0.02$, $\sigma_p = 0.3$, $\sigma_i = 0.5$, $\sigma_b = 0.002$, and $\kappa = 6$.

Figure 3 shows the variation of critical Mach number, M_0, maximum Mach number, M_{max}, and maximum value of the potential, ϕ_{max}, for electron-acoustic mode for the normalized parameters: $n_{i0} = 0.05$, $n_{b0} = 0.02$, $\sigma_p = 0.3$, $\sigma_i = 0.5$, $\sigma_b = 0.002$, and $\kappa = 6$. Electron-acoustic mode supports only negative potential soliton. We see that both M_0 and M_{max} increases with the increase in V_{b0}. The limitation on the maximum attainable amplitude is attributed to the requirement of the number density of beam electrons, n_b, to remain real valued.

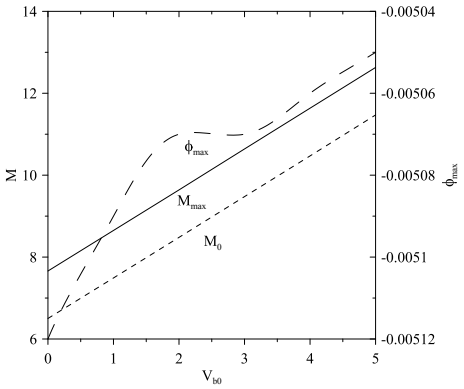

Figure 3. Variation of critical Mach number, M_0 (dashed curves), maximum Mach number, M_{max}, and maximum value of potential, ϕ_{max} (long-dashed curve), with V_{b0} for electron-acoustic mode for the normalized parameters: $n_{i0} = 0.05$, $n_{b0} = 0.02$, $\sigma_p = 0.3$, $\sigma_i = 0.5$, $\sigma_b = 0.002$, and $\kappa = 6$. Here the Y-axis on the left hand side (L.H.S) shows the scale for Mach number, while on the right hand side (R.H.S) shows the scale for maximum electric potential amplitude, ϕ_{max}.

4 Conclusions

We apply our theoretical model to explain the electrostatic waves observed by the ARTEMIS mission during its first lunar wake flyby on 13 February 2010 [1]. For numerical estimation of the physical properties of the electrostatic waves, we have used the parameters: temperature of electron, T_e=28eV and total number density, n_0=0.13 cm^{-3}. For these parameters, the ion-acoustic speed, C_a=52 km s^{-1}, the effective hot Debye length, λ_{de}=109 m, and the effective proton plasma frequency, f_{pp}=474.69 Hz.

In Table I, the unnormalized soliton velocity (V), electric field (E), the soliton width (W) and peak frequency, f_{peak} corresponding to the maximum power in the fast Fourier transform (FFT) power spectra for various V_{b0} values are given for slow and fast ion-acoustic solitons and electron-acoustic solitons. Here, the width, W, is defined as the full width at half maximum.

In Table 1, the higher values of the width correspond to the lower soliton velocity. We note from the table that the velocity of the electron-acoustic soliton is the highest fol-

Table 1. Properties of slow and fast ion-acoustic solitons and electron-acoustic solitons for various values of V_{b0} for the normalized parameters: $n_{i0} = 0.05$, $n_{b0} = 0.02$, $\sigma_p = 0.3$, $\sigma_i = 0.5$, $\sigma_b = 0.002$, and $\kappa = 6$. Here, the temperature of electron, T_e=28eV and total number density, n_0=0.13 cm^{-3}, are used for the numerical estimation of the relevant properties.

Mode	V_{bo}	Polarity	V (Km s^{-1})	E (mV m^{-1})	W(m)	f_{peak} (Hz)
Slow ion-acoustic	1	+ve	32.04-32.15	0.0002-0.012	1086.43-207.25	10.76-43.15 $(0.003-0.013)f_{pe}$
	5	-ve	30.31-31.24	0.0002-0.06	2048.50-178.89	6.79-55.98 $(0.002-0.017)f_{pe}$
Fast ion-acoustic	1	+ve	54.36-58.29	0.0008-2.23	2506.63-231.25	12.16-78.34 $(0.004-0.024)f_{pe}$
	5	-ve	43.85-45.71	0.0004-0.034	1084.24-170.16	14.72-81.85 $(0.004-0.024)f_{pe}$
Electron-acoustic	1	-ve	390.34-447.81	0.004-0.42	2292.84-403.59	87.3-300.61 $(0.027-0.09)f_{pe}$
	5	-ve	597.42-653.86	0.006-0.42	1854.34-410.137	133.66-439.54 $(0.04-0.14)f_{pe}$

lowed by fast ion-acoustic soliton and then by slow ion-acoustic soliton. On the basis of the observations made by ARTEMIS mission during its first lunar wake flyby on 13 February 2010, Tao et al. [1] reported that the frequency range of the observed electrostatic waves lies mostly between $0.1f_{pe}$ and $0.4f_{pe}$. However, in the middle of the flyby the power was found to be as low as $0.01f_{pe}$, f_{pe} is the electron plasma frequency (f_{pe}=3237.78 Hz). Further, they reported that the electric field amplitude parallel to the ambient magnetic field roughly varies from 5 to 15 mV m^{-1}. From Table 1 we can see that for both slow and fast ion-acoustic solitons the peak frequency corresponding to the higher velocity soliton is closer to the observed low-frequency of $\sim 0.01f_{pe}$. In case of electron-acoustic solitons the frequency corresponding to maximum velocity matches with the observed high frequency value $\sim 0.1f_{pe}$. Further, we note that the frequency of the electron-acoustic soliton increases with V_{b0}. The electric field amplitude of both slow ion-acoustic soliton and electron-acoustic soliton is lesser than the reported value. While the electric field amplitude of the fast ion-acoustic soliton corresponding to the higher velocity value is closer to the reported value of ~ 5 mV m^{-1}. However, it is found that with increasing values of V_{b0}, the soliton properties matches with the observed values. The slow and fast ion-acoustic solitons can explain the observed low-frequency waves $\sim 0.01f_{pe}$. While the electron-acoustic soliton can explain the observed high-frequency waves $\sim 0.1-0.4f_{pe}$.

5 Acknowledgements

GSL thanks the National Academy of Sciences, India for the support under the NASI-Senior Scientist Platinum Jubilee Fellowship scheme.

References

[1] J. B. Tao, R. E. Ergun, D. L. Newman, J. S. Halekas, L. Andersson, V. Angelopoulos, J. W. Bonnell, J. P. McFadden, C. M. Cully, H. U. Auster, K. H. Glassmeier, D. E. Larson, W. Baumjohann, and M. V. Goldman, "Kinetic Instabilities in the Lunar Wake: ARTEMIS Observations", *J. Geophys. Res.*, **117**, 28, March 2012, A03106, doi:10.1029/2011JA017364.

[2] K. Hashimoto, M. Hashitani, Y. Kasahara, Y. Omura, M. N. Nishino, Y. Saito, S. Yokota, T. Ono, H. Tsunakawa, H. Shibuya, M. Matsushima, H. Shimizu, and F. Takahashi, "Electrostatic Solitary Waves Associated with Magnetic Anomalies and Wake Boundary of the Moon Observed by KAGUYA", *Geophys. Res. Lett.*, **37**, 6, October 2010, L19204, doi:10.1029/2010GL044529.

[3] G. S. Lakhina, S. V. Singh, A. P. Kakad, and J. S. Pickett, "Generation of Electrostatic Solitary Waves in the Plasma Sheet Boundary Layer", *J. Geophys. Res.*, **116**, 19, October 2011, A10218, doi:10.1029/2011JA016700.

[4] G. S. Lakhina, and S. V. Singh, "Generation of Weak Double Layers and Low-Frequency Electrostatic Waves in the Solar Wind", *Solar Phys.*, **290**, 2016, 15, September 2015, pp. 3033-3049, doi:10.1007/s11207-015-0773-1.

[5] D. Summers, and R. M. Thorne, "The Modified Plasma Dispersion Function", *Phys. of Fluids B: Plasma Phys.*, **3**, 8, April 1991, pp. 1835-1847, doi:10.1063/1.859653.